View metadata, citation and similar papers at core.ac.uk
brought to you by CORE
provided by UCL Discovery

Positron Plasma Diagnostics and Temperature Control for Antihydrogen Production

M. Amoretti,[1] C. Amsler,[2] G. Bonomi,[3] A. Bouchta,[3] P. D. Bowe,[4] C. Carraro,[1,5] C. L. Cesar,[6] M. Charlton,[7] M. Doser,[3] V. Filippini,[8] A. Fontana,[8,9] M. C. Fujiwara,[10] R. Funakoshi,[10] P. Genova,[8,9] J. S. Hangst,[4] R. S. Hayano,[10] L. V. Jørgensen,[7] V. Lagomarsino,[1,5] R. Landua,[3] D. Lindelöf,[2] E. Lodi Rizzini,[11] M. Macrí,[1] N. Madsen,[2] G. Manuzio,[1,5] P. Montagna,[8,9] H. Pruys,[2] C. Regenfus,[2] A. Rotondi,[8,9] G. Testera,[1,*] A. Variola,[1] and D. P. van der Werf[7]

(ATHENA Collaboration)

[1]*Istituto Nazionale di Fisica Nucleare, Sezione di Genova, 16146 Genova, Italy*
[2]*Physik-Institut, Zürich University, CH-8057 Zürich, Switzerland*
[3]*EP Division, CERN, CH-1211 Geneva 23, Switzerland*
[4]*Department of Physics and Astronomy, University of Aarhus, DK-8000 Aarhus C, Denmark*
[5]*Dipartimento di Fisica, Università di Genova, 16146 Genova, Italy*
[6]*Instituto de Fisica, Universidade Federal do Rio de Janeiro, Rio de Janeiro 21945-970, Brazil, and Centro Federal de Educação Tecnologica do Ceara, Fortaleza 60040-531, Brazil*
[7]*Department of Physics, University of Wales–Swansea, Swansea SA2 8PP, United Kingdom*
[8]*Istituto Nazionale di Fisica Nucleare, Sezione di Pavia, 27100 Pavia, Italy*
[9]*Dipartimento di Fisica Nucleare e Teorica, Università di Pavia, 27100 Pavia, Italy*
[10]*Department of Physics, University of Tokyo, Tokyo 113-0033, Japan*
[11]*Dipartimento di Chimica e Fisica per l'Ingegneria e per i Materiali, Università di Brescia, 25123 Brescia, Italy, and Istituto Nazionale di Fisica Nucleare, Gruppo collegato di Brescia, 25123 Brescia, Italy*

(Received 14 February 2003; published 31 July 2003)

Production of antihydrogen atoms by mixing antiprotons with a cold, confined, positron plasma depends critically on parameters such as the plasma density and temperature. We discuss nondestructive measurements, based on a novel, real-time analysis of excited, low-order plasma modes, that provide comprehensive characterization of the positron plasma in the ATHENA antihydrogen apparatus. The plasma length, radius, density, and total particle number are obtained. Measurement and control of plasma temperature variations, and the application to antihydrogen production experiments are discussed.

DOI: 10.1103/PhysRevLett.91.055001 PACS numbers: 52.27.Jt, 36.10.–k, 52.35.Fp, 52.70.–m

The ATHENA Collaboration recently produced and detected cold antihydrogen atoms [1] at the CERN Antiproton Decelerator. A similar result has been subsequently reported by the ATRAP Collaboration [3]. The antihydrogen was made by mixing low energy antiprotons with a cold, dense positron plasma in a nested Penning trap [4]. A knowledge of the characteristics of the positron plasma is important for several reasons. The most likely antihydrogen formation mechanisms, spontaneous recombination and three-body recombination, have different dependences on both the density and the temperature of the positron plasma [5]. Knowing these parameters is crucial in helping to elucidate the antihydrogen formation mechanism. Control and simultaneous monitoring of the positron plasma temperature allow the antihydrogen formation reaction to be effectively turned off while maintaining overlap between antiprotons and positrons. This provides a good measurement of the total background signal for our unique antihydrogen detector [1]. Furthermore, the space charge potential of a sufficiently dense (10^8 cm^{-3}) and extensive (length 3 cm) positron plasma considerably alters the effective electrostatic potential in the positron trap and thus the dynamics of the antiprotons in the nested trap.

Harmonically confined one component plasmas at temperatures close to absolute zero are known to form spheroids of constant charge density [6]. In our case the shape is a prolate ellipsoid characterized by the aspect ratio $\alpha = z_p/r_p$, where z_p and r_p are the semimajor axis and semiminor axis, respectively [Fig. 1(a)]. A cold fluid theory [7] relating the frequencies of the low-order plasma modes to the density and the aspect ratio of spheroidal plasmas was confirmed experimentally for laser cooled ion plasmas [8,9] and successfully applied to cold electron plasmas [10]. Work on finite temperature electron plasmas demonstrated that mode detection could be used as a diagnostic of density and aspect ratio and that for a plasma of known density and aspect ratio the frequency of the quadrupole mode is dependent on the plasma temperature [11,12].

Here we describe an extension to the above work which provides a nondestructive diagnostic based on measurements of the first two axial modes of a finite temperature positron plasma. The diagnostic has no discernible effect

 © 2003 The American Physical Society

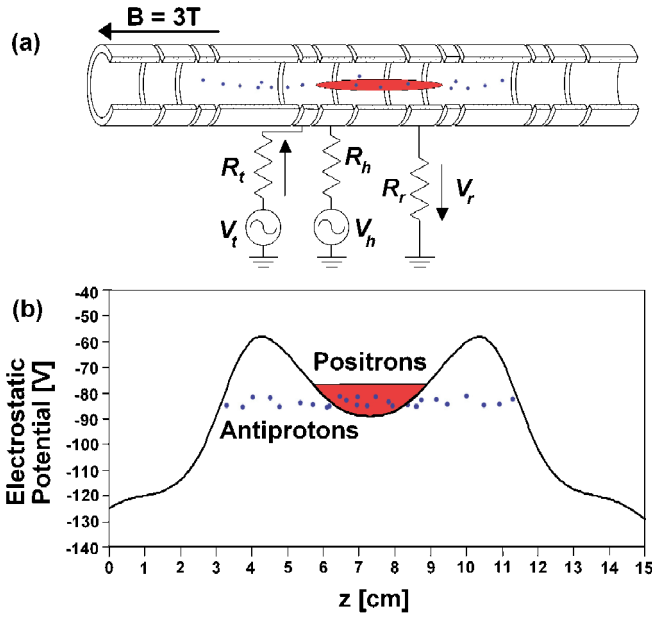

FIG. 1 (color online). (a) Trap electrodes with the heating and mode detection electronics. The shape of the positron plasma prolate ellipsoid is shown schematically. (b) The axial potential of the ATHENA nested trap is shown and the ranges of axial motion of the positrons and the antiprotons indicated schematically.

on the normal evolution of the plasma, so it can be used during antihydrogen production. We have developed a model in which the plasma length can be extracted from the shape of the resonance when the dipole mode is excited. Thus the aspect ratio, density, and length can be measured and the radius and positron number obtained. We show that we can monitor induced changes in the temperature while ensuring that the normal evolution of other plasma parameters is not changed. Using this monitor and suitable radio-frequency excitation of the dipole mode we can set the plasma temperature during the interaction between positrons and antiprotons.

In ATHENA, the positrons and antiprotons are confined by cylindrical electrodes of radius $r_w = 1.25$ cm. These are inserted in a cryostat and immersed in a 3 T magnetic field. The positrons are held in the central part of the trap by a harmonic axial potential [see Fig. 1(b)]. In the high magnetic field the positrons cool by synchrotron radiation [13]. We have not measured the temperature of the positron plasma but note that the lower limit is set by the temperature of the trap electrodes (15 K).

The first two axial modes (dipole and quadrupole modes) are excited by applying a sinusoidal perturbation to one electrode with an electromotive force $V_t = v_t e^{j\omega t}$. The oscillation of the plasma induces a current in the pickup electrode [14,15] and a voltage $V_r = v_r(\omega)e^{j\omega t}$ is detected across the resistance R_r [Fig. 1(b)]. Experimentally the ratio $T_L(\omega) = v_r(\omega)/v_t$ is measured as a function of the drive frequency ω by means of a network analyzer. A narrow stepwise frequency sweep is made of the voltage source across the resonance frequency of each mode. The excitation amplitude v_t is of the order of 100 μV and the dwell time for each 5 kHz step is 3.96 ms. The number of scan steps is usually 50. The choice of scan width is a balance between following scan-to-scan changes in mode frequency and avoiding perturbations to the normal evolution of the plasma. To follow changes in the plasma over a longer time scale an automatic frequency tracking code has been implemented to allow the excitation to be locked to the mode frequencies. For each frequency step, the amplitude and phase (relative to that of the driving signal) of the voltage induced by the plasma motion are acquired. The cross talk signal between the transmitting and receiving electrodes is acquired without positrons and subtracted from the signal measured with the plasma present.

The plasma number density n and aspect ratio α can be extracted from the zero-temperature analytical model [7] using the measured frequencies (ω_1, ω_2) of the dipole and quadrupole modes. We have developed an equivalent circuit model which explicitly includes the plasma dimensions. This method yields directly the plasma length when α and n are known. In contrast, other equivalent circuit approaches utilizing tuned circuits and assuming small cloud dimensions measured the total number of particles in Penning traps [15]. Our model describes the signal induced on an electrode by the coherent oscillations of the dipole mode when an external driving force is applied. In particular, we write [16]

$$T_L = \frac{g_t(\alpha, z_p) g_r(\alpha, z_p) R_r}{R_s + j\omega L(1 - \omega_1^2/\omega^2)}. \quad (1)$$

The dimensionless functions g_r and g_t depend on the shape of the plasma and on the geometry of the trap. They describe the effects of the finite plasma extension both on the mode excitation and detection. $g_t(\alpha, z_p)V_t/2r_w$ is the electric field acting on the center of mass of the plasma when the dipole mode is excited by applying a voltage V_t to the transmitting electrode with the other electrodes grounded. The function $g_r(\alpha, z_p)$ is related to the current I_r induced by the dipole mode oscillation on the receiving electrode, $I_r = Neg_r(\alpha, z_p)v_{cm}/2r_w$, where v_{cm} is the velocity of the particles due to the dipole mode and e is the positron (electron) charge. T_L is obtained by measuring $T'_L = AT_L$, where A is the net gain of the electronics chain and it is independent of the plasma properties. We used electrons to fine-tune this parameter by comparing the number obtained by this diagnostic with the number measured on a Faraday cup. Electrons were chosen as they can be loaded faster, with a wider range of total number N. The inductance L of the equivalent circuit is related to the plasma length,

$$L = \frac{3\alpha^2 r_w^2 m}{\pi n e^2 z_p^3}, \quad (2)$$

where m is the positron (or electron) mass [16]. The resistance R_s characterizes the damping rate of the mode. α and n are determined independently by the frequency analysis. The power transmitted through the plasma $|T_L|^2$ is related to R_s and z_p by Eqs. (2) and (1). Thus a fit to the measured transmitted power yields z_p. The radius r_p and the total number N can now be found. An example of an application of this diagnostic to positrons is shown in Fig. 2. Here the total number obtained with the model is plotted against the number found by extraction to a Faraday cup. In this regime the linearity and good correspondence in the absolute number show that both the model and its implementation constitute a complete, real-time, nondestructive plasma diagnostic. Typical properties of the ATHENA positron plasma for antihydrogen production were 7×10^7 positrons at a density of about 1.7×10^8 cm^{-3} in a plasma ≈ 3.2 cm long ($2z_p$) with a radius of about 0.25 cm and a storage time of several hundreds of seconds. The maximum change in the plasma parameters during the mixing cycle of 190 s was less than 10%.

Because of the importance of temperature in antihydrogen production, we have also investigated whether this diagnostic system can be used to detect changes in the plasma temperature. Previous authors have demonstrated, with work on similar electron plasmas [11,12], that temperature changes manifest themselves in frequency shifts of the quadrupole mode. In particular, they find

$$k\Delta T = \frac{mz_p^2}{5}[(\omega_2^h)^2 - (\omega_2)^2]\left[3 - \frac{\omega_p^2\alpha^2}{2\omega_2^2}\frac{d^2f(\alpha)}{d\alpha^2}\right]^{-1}, \quad (3)$$

where $f(\alpha) = 2Q_1(\alpha/\sqrt{\alpha^2 - 1})/(\alpha^2 - 1)$ and Q_1 is a Legendre function of the second kind, ω_2^h is the quadrupole frequency with heating applied, and ω_p is the plasma frequency. The values of α, ω_p, and z_p are evaluated in the cold fluid limit. Provided that these parameters do not vary significantly when the plasma temperature changes, a measured shift in the quadrupole frequency can be used to calculate the magnitude of the temperature change.

We have used the mode diagnostic system to investigate the response of a cold and dense positron plasma without antiprotons to heating, implemented by applying an excitation near the dipole frequency (21 MHz) to one of the trap electrodes [Fig. 1(a)]. Off-resonance heating pulses were not effective. The excitation is a variable amplitude signal that is swept from 20 to 22 MHz at a repetition rate of about 1 kHz. This is done to ensure that the dipole mode frequency is covered and that the plasma reaches thermal equilibrium. Previous authors report an equilibration rate of some tens of kHz in similar conditions [17]. Figure 3 shows the behavior of the quadrupole frequency when the initially cold plasma is subjected to heat off-on cycles. Application of the excitation results in a rapid, voltage-dependent rise in the quadrupole frequency. When the excitation is removed, the quadrupole frequency returns to a value in step with the evolution of the unperturbed plasma which is also shown in Fig. 3. The unperturbed plasma evolution is characterized by a slow decrease in the frequency of the quadrupole mode and corresponding decrease in aspect ratio and density. This is consistent with a slow expansion of the plasma. The heating and the cooling times are faster than our

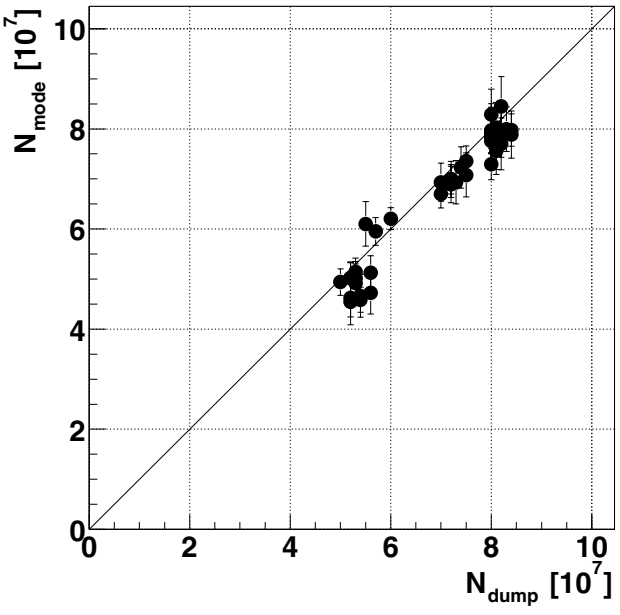

FIG. 2. The total number of positrons obtained using the modes diagnostic is plotted against the number obtained by extracting the positrons to a Faraday cup.

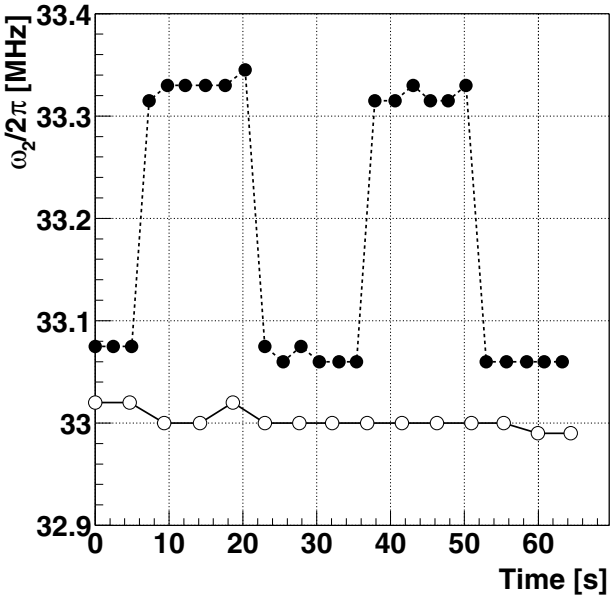

FIG. 3. The quadrupole mode frequency versus time for normal evolution (○) and for two heat off-on cycles (●). The frequency shift corresponds to an increase of the plasma temperature of about 150 meV.

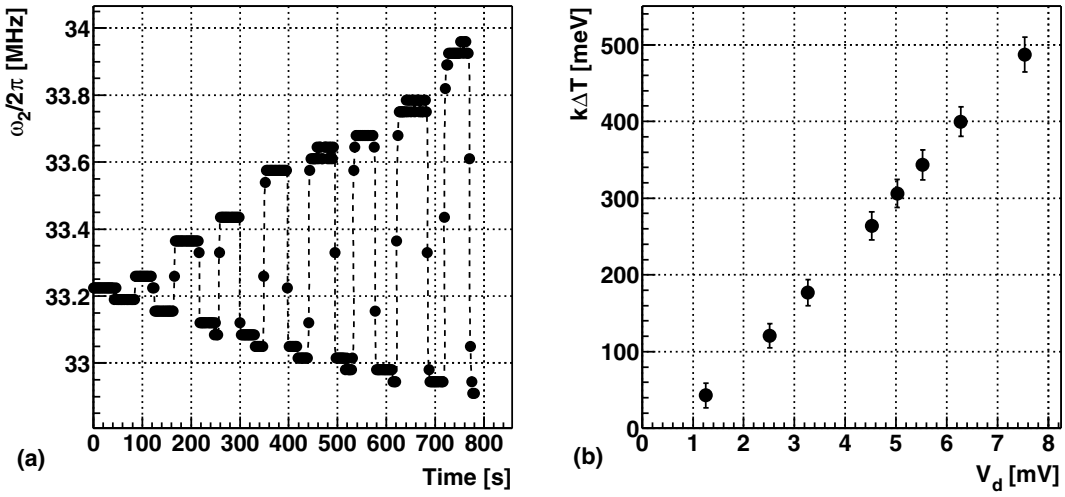

FIG. 4. (a) Time evolution of the quadrupole mode frequency during a heating off-on cycle. The different frequency shifts correspond to different heating amplitudes V_d. The drift of the frequency in the unperturbed intervals is due to the plasma expansion, and it is consistent with the normal evolution of the unperturbed plasma (see also Fig. 3). (b) Dependence of the temperature variation on radio-frequency signal amplitude for the same cycle.

sampling interval resulting in the observed discontinuities of the frequency shifts on the time scale of Fig. 3.

Furthermore, for these heating amplitudes, without antiprotons we observe no discernible positron loss with our positron annihilation detector which covers a solid angle of 80% of 4π [18]. Figure 4(a) shows the response of the plasma quadrupole frequency during heat off-on cycles with different amplitudes V_d of generated heating voltage [directly proportional to V_h of Fig. 1(a)]. Thus the dependence of temperature increase ΔT on V_d was found, and the result is shown in Fig. 4(b). For the data reported here the minimum measurable temperature was about 15 meV due to the frequency step size used (20 kHz). The minimum step size of 5 kHz would give a sensitivity of a few meV. The observed linear dependence of the temperature rise on V_d is in contrast with the linear dependence on the power (and thus on V_d^2) that one would expect. This could be most likely due to nonlinear effects of the on-resonance heating. A nonlinear regime could also explain the fact that the temperature rise in Fig. 4(b) appears to extrapolate to zero at finite V_d.

The utility of the mode diagnostic system as applied to antihydrogen production is immediately apparent if we consider that the radiative reaction rate is proportional to n and to $T^{-1/2}$, while the three-body reaction rate varies as n^2 and $T^{-9/2}$ [5]. In order to gain insight into the experimental production mechanism and to ensure reproducible results, careful monitoring of any changes in these parameters is essential. The ability to reproducibly add heat to the positron plasma, and to thereby control the reaction rate, is also very desirable. We have already utilized the heating and temperature diagnostic to "turn off" antihydrogen production in ATHENA [1], providing a useful null measurement.

The implementation of automated mode analysis measurement has allowed us to log the plasma parameters at all times when positrons are in the trap. The system is wideband and does not require that any resonant circuitry be mounted internally on trap electrodes. We are thus free to choose a wide range of depths for our harmonic positron trap and are therefore able to tune the shape of our positron plasma at will. Knowing the size of the positron cloud is crucial to assuring a good spatial overlap between antiprotons and positrons in the reaction region. The space charge potential of our positron plasma flattens the potential inside its volume along the z direction reducing the potential barrier seen by the antiprotons in the mixing trap by several volts. Information about the effective potential is important in helping to understand the antiproton cooling and interaction dynamics.

We have extended the plasma mode diagnostic method to provide comprehensive characterization of a cold, dense positron plasma employed in the ATHENA antihydrogen experiment. The method has already been utilized to great advantage in ATHENA and promises to be an essential element of future experiments. The technique, while particularly useful for nondestructive measurements on difficult-to-produce species such as positrons, has immediate applicability to other Penning trap plasmas.

This work was supported by INFN (Italy), CNPq and FAPERJ (Brazil), MEXT (Japan), SNF (Switzerland), SNF (Denmark), and EPSRC (United Kingdom).

*Corresponding author.
Electronic address: testera@infnge.ge.infn.it

[1] M. Amoretti *et al.*, Nature (London) **419**, 456 (2002).
[2] S. Maury, Hyperfine Interact. **109**, 43 (1997).
[3] G. Gabrielse *et al.*, Phys. Rev. Lett. **89**, 213401 (2002).
[4] G. Gabrielse, S. L. Rolston, L. Haarsma, and W. Kells, Phys. Lett. A **129**, 38 (1988).
[5] M. H. Holzscheiter and M. Charlton, Rep. Prog. Phys. **62**, 1 (1999), and references therein.
[6] L. Turner, Phys. Fluids **30**, 3196 (1987).
[7] D. H. E. Dubin, Phys. Rev. Lett. **66**, 2076 (1991).
[8] D. J. Heinzen *et al.*, Phys. Rev. Lett. **66**, 2080 (1991).
[9] J. J. Bollinger *et al.*, Phys. Rev. A **48**, 525 (1993).
[10] C. S. Weimer, J. J. Bollinger, F. L. Moore, and D. J. Wineland, Phys. Rev. A **49**, 3842 (1994).
[11] M. D. Tinkle *et al.*, Phys. Rev. Lett. **72**, 352 (1994); M. D. Tinkle, R. G. Greaves, and C. M. Surko, Phys. Plasmas **2**, 2880 (1995).
[12] H. Higaki *et al.*, Phys. Rev. E **65**, 046410 (2002).
[13] T. M. O'Neil, Phys. Fluids **23**, 725 (1980).
[14] C. A. Kapetanakos and A.W. Trivelpiece, J. Appl. Phys. **42**, 4841 (1971).
[15] D. J. Wineland and H. G. Dehemelt, J. Appl. Phys. **46**, 919 (1975); X. Feng *et al.*, J. Appl. Phys. **79**, 8 (1996).
[16] M. Amoretti *et al.*, Phys. Plasmas 10, 3056 (2003).
[17] B. R. Beck, J. Fajans, and J. H. Malmberg, Phys. Plasmas **3**, 1250 (1996).
[18] C. Regenfus, Nucl. Instrum. Methods Phys. Res., Sect. A **501**, 65 (2003).